Advanced Composites and Hybrid Materials (2022) 5:1017–1029
https://doi.org/10.1007/s42114-022-00478-3

ORIGINAL RESEARCH

Electrospun structural nanohybrids combining three composites for fast helicide delivery

Hang Liu[1] · Haibin Wang[2] · Xuhua Lu[2] · Vignesh Murugadoss[3,4] · Mina Huang[4,5] · Haisong Yang[6] · Fuxian Wan[7] · Deng-Guang Yu[1] · Zhanhu Guo[4]

Received: 14 February 2022 / Revised: 25 March 2022 / Accepted: 24 April 2022 / Published online: 30 May 2022

Abstract

The effective and convenient delivery of poorly water-soluble drugs often needs a combined effort of several disciplines. In this study, a brand-new structural hybrid, tri-section Janus nanofiber (TJN), was successfully prepared using a tri-fluid electrospinning and was demonstrated to be useful for delivering helicide, a poorly water-soluble Chinese herbal medicine. The TJNs were composed of three sorts of polymer-based nanocomposites: helicide-polyvinylpyrrolidone (PVP), sodium dodecyl sulfate (SDS)-PVP, and sucralose-PVP. The electrospinning processes, characterized by a new homemade spinneret, were investigated to disclose the TJNs' micro-formation mechanism. SEM and TEM results verified that the TJNs presented in the linear morphologies and the three sections within the nanofibers could be discerned clearly. XRD and ATR-FTIR showed that the functional ingredients, helicide, SDS, and sucralose, presented in their own sections in an amorphous state due to the favorable secondary interactions with the PVP matrices. Three methods were carried out to study the functional performances of TJNs. The results showed that not only the helicide was able to dissolve all at once, but also the loaded SDS and sucralose were able to be released before helicide for a sequential release effect and thus for a potential convenient and effective drug delivery to the patients through tongue mucosas. The TJN can be a useful platform for supporting the developments of advanced functional nanomaterials and multiple-functional biomaterials.

Keywords Nanohybrids · Nanocomposites · Janus nanofibers · Tri-fluid electrospinning · Drug delivery · Poorly water-soluble drug

1 Introduction

During the past half a century's developments of pharmaceutics, the polymers are increasingly demonstrated to be the backbone for supporting new kinds of drug delivery systems (DDSs) [1–4]. Initially, properties of polymers are successfully exploited to modify the drug release profiles for an effective, safe, and convenient therapeutic action [5–7]. For example, the insoluble and degradable polymers are frequently exploited to develop drug sustained or extended release through a diffusion mechanism in the formats of

Hang Liu and Haibin Wang contributed equally to this work.

✉ Xuhua Lu
xuhualu@hotmail.com

✉ Deng-Guang Yu
ydg017@usst.edu.cn

✉ Zhanhu Guo
zguo10@utk.edu

[1] School of Materials and Chemistry, University of Shanghai for Science and Technology, Shanghai 200093, China

[2] Department of Orthopaedics, Shanghai Changzheng Hospital, Naval Medical University, Shanghai 200003, China

[3] Advanced Materials Division, Engineered Multifunctional Composites (EMC) Nanotech LLC, Knoxville, TN 37934, USA

[4] College of Materials Science and Engineering, Taiyuan University of Science and Technology, Taiyuan 030024, China

[5] Integrated Composites Laboratory (ICL), Department of Chemical and Bimolecular Engineering, University of Tennessee, Knoxville, TN 37996, USA

[6] Department of Orthopaedics, Second Affiliated Hospital of Naval Medical University, Shanghai 200433, China

[7] College of Chemistry and Material Science, Shandong Agricultural University, Tai'an 271018, China

nanoparticles, nanofibers, and also bulk materials [8–10]. Hydrophilic and water-soluble polymers are always utilized to enhance the solubility and to accelerate the dissolution rates of poorly water-soluble drugs and also to develop the DDSs for providing the immediate or pulsatile drug release profiles [11–13]. However, how these DDSs show the desired functional performances has a close relationship with the drug-polymer co-existing status and the related materials engineering methods [14–16].

The drug presents in the polymer matrix mainly in the following formats: separate (such as depots in the inner section or nano crystals on the surface) [17, 18]; homogeneous distribution all over the polymeric carriers [19, 20]; and heterogeneous distributions (such as gradual distribution and discrete distribution) [21–23]. Among these co-existing manners, the most frequent type is the homogeneous distribution, by which the polymeric carriers' properties are greatly exploited for the desired functional performances [24, 25]. These homogeneous products are often called polymer-based composites (as an opposite of hybrids, which often have separated phases within the subjects) or often solid dispersion in pharmaceutics [26–28]. How to make the drug molecules uniformly distribute all over the polymeric matrices comprises a big challenge to the researchers in the fields of pharmaceutics, materials science, nano science, and polymer engineering.

Electrospinning, as its peer electrospraying, is an electrohydrodynamic technique and initially a method for creating polymeric nanofibers [29–32]. The polymers that are applied for drug delivery and have fine electrospinnability are slightly over one hundred in literature [33, 34]. However, there are numerous polymer-based composites that are generated using electrospinning [35–37]. This contrast should have a close relationship with the capability of electrospinning in creating a wide variety of nanofibers with various loaded ingredients for functional applications. Initially, electrospinning is popular with the advent of this nano era due to a top-down, straightforward, and facile manner for creating nano products [38–41]. However, with the developments of this technique, its capability of generating nanofibers is fast expanded along several directions: (1) filament-forming polymers or some little molecules, typically lipid and β-cyclodextrin (CD), can be electrospun into nanofibers [42–44]; (2) the generation of multiple-chamber nanostructures in a single step using the multiple-fluid electrospinning, which is impossible for other top-down methods and also very difficult for most bottom-up methods such as molecular self-assembly [45, 46]; (3) the applications of materials without electrospinnability for producing nanofibers directly, i.e., working fluids without electrospinnability can be converted into nanofibers when they are treated simultaneously with electrospinnable polymer solution [47–50]; and (4) the applications of electrospun polymeric nanofibers as templates for creating other kinds of products, such as ceramics and other inorganic nanofibers from the after-treatment of the polymer-based nanofibers [51–55].

As for the multiple-fluid electrospinning and the related multiple-chamber structures, the most common one is coaxial electrospinning and its main products core-sheath nanofibers [56–62]. From the first reports about coaxial electrospinning [63], today there are 4356 publications (with "TS = coaxial electrospinning or core–shell nanofibers or core-sheath nanofibers" to search in Web of Science in 27-Jan-2022) about this processes and the corresponding core-sheath structures. Additionally, Dzenis once pointed out that coaxial electrospinning was one of the most important break points in this field [64]. What is more, along this way, tri-axial (abbreviation of tri-layer coaxial) and quad-axial electrospinning are successively reported in literature, and the related multi-layer core-sheath nanostructures were clearly demonstrated [25, 65–69]. However, a sharp contrast is that the investigations about side-by-side electrospinning and the related Janus nanofibers are extremely limited [70, 71]. The found literature in Web of Science is only 269 (with "TS = side-by-side electrospinning or Janus nanofibers" to search in Web of Science in 27-Jan-2022), and in which half of them are review papers. This has a close relationship with the difficulties of creating Janus nanofibers using two metal capillaries in a parallel manner as the spinneret. The same charge of two working fluids makes it inevitable that they separate from each other due to the repelling, when they are pumped out from the outlets of a spinneret nozzle. In turn, this phenomenon would result in the failure of creating Janus nanofibers with integrated side-by-side (or Janus) structures [72, 73].

To solve this issues, an eccentric spinneret was recently reported, which is characterized by two capillaries with one relied on the inner wall of another capillary [74, 75]. This spinneret is demonstrated to be effective for preventing the separation of two parallel working fluids due to the following reasons. One is that the two fluids were formed a full and whole circle for being charged, just as the concentric spinneret. The other is that the two working fluids can contact with each other through an enlarged surface area, not a point contact in the two-parallel metal capillary format. Later, this method was further improved by exploiting a third solvent to keep the drawing and drying processes simultaneously for creating Janus nanofibers with an integrated inner Janus structure [76, 77]. Inspired by this strategies and the related electrohydrodynamic knowledge, the parallel pumping of 3 or even 4 working fluids to the electrical fields should be possible for creating the 3-section Janus or even 4-section Janus nanofibers.

In this study, a brand-new tri-fluid electrospinning process is developed, which is characterized by a new structural spinneret. The electrospun tri-section Janus nanofibers (TJNs) contained helicide (a poorly water-soluble drug model), sodium dodecyl sulfate (SDS, a trans-membrane enhancer), and sucralose (a sweeter) in their owns' polymer-based nanocomposites. The TJNs can be exploited for drug delivery through oral mucosa for realizing fast dissolution and rapid permeation for a therapeutic action, and meanwhile, a sequentially controlled release of them can ensure a convenient and compliant administration to the patients.

2 Materials and methods

2.1 Materials

Helicide (98% purity, 4-Formylphenyl beta-D-Allopyranoside) was received from Xi'an boliante Chemical Co., Ltd. (Xi'an, China). Two polymeric matrices of polyvinylpyrrolidone (PVP K 60, M_w = 360,000 and PVP K10, M_w = 8,000) were purchased from Sigma-Aldrich Corp. (Shanghai, China). Sodium dodecyl sulfate (SDS), *N,N*-dimethylacetamide (DMAc), anhydrous ethanol, methylene blue, and basic fuchsin were bought from Sinopharm group (Shanghai, China) and were used as received.

2.2 Preparation of TJNs

After some pre-experiments, three working fluids were prepared for implementing the tri-fluid side-by-side electrospinning to prepare the TJNs.

Fluid 1: 10.0 g PVP K60 and 4.0 g helicide were co-dissolved into 100 mL solvent mixture of ethanol and DMAc in a volume ratio of 7:3 (for optimizing the experimental conditions, 0.01 g methylene blue was added).
Fluid 2: 20.0 g PVP K10 and 10.0 g sucralose were co-dissolved into 100 mL ethanol (for optimizing the experimental conditions, 0.01 g basic fuchsin was added).
Fluid 3: 10.0 g PVP K60 and 0.5 g SDS were co-dissolved into 100 mL 80% (v/v) ethanol aqueous solution.

A homemade spinneret was developed to build a tri-fluid electrospinning system, which was explored for creating the TJNs. The fluid flow rates (mL/h) were fixed at 1.0:1.0:0.5 (Fluid 1:Fluid 2:Fluid 3). The applied voltage was fixed at 11.0 kV. The nanofiber deposition distance was fixed at 20 cm. The collected TJNs were kept at a vacuum drying oven for characterization.

2.3 Characterization of properties

2.3.1 Morphology and structure analyses

The morphology of electrospun TJNs was observed using a field emission scanning electron microscopy (SEM, FEI Quanta450FEG, USA). Their cross-sections were prepared by inserted a piece of TJNs into liquid nitrogen for 20 min and later broken manually. The samples for SEM were gold sputter-coated for 1.5 min under N_2 atmosphere. The fibers' diameters were estimated using ImageJ software (National Institutes of Health, USA) by analyzing over 100 fiber places in SEM images. The tri-section Janus structures of nanofibers were also assessed using a transmission electron microscope (TEM, JEM 2100F, JEOL, Tokyo, Japan).

2.3.2 State of the loaded components and their compatibility

An X-ray diffractometer (Bruker-AXS with Cu Kα radiation, Karlsruhe, Germany) was utilized for conducting X-ray diffraction (XRD) analyses. The experimental conditions: an applied voltage of 40 kV, a current of 30 mA, and a 2θ range from 5 to 60°. A Spectrum 100 FTIR Spectrometer (Perkin-Elmer, Billerica, USA) was exploited to implement the attenuated total reflectance-Fourier transform infrared (ATR-FTIR) measurements at a resolution of 2 cm^{-1} and at a range from 4000 to 500 cm^{-1}.

2.4 Functional performances

2.4.1 Drug loading efficiency

The helicide concentration was measured using a UV–vis spectrophotometer (UV-2102PC, Unico Instrument Co., Ltd. Shanghai, China). The standard equation between the helicide concentration (C, μg/mL) and absorbance (A) was A = 0.117C-0.014 (R = 0.9996), which was built at the maximum absorbance at λ_{max} = 270 nm and within a linear range of 0.0 to 25.0 μg/mL.

For determining the encapsulation efficiency (EE, %) of helicide in the TJNs from the tri-fluid electrospinning, an amount of 10.0 mg TJNs were dissolved into 500 mL distilled water. After detection of the solutions, the detected helicid content (C_D) can be calculated from the standard equation, and the EE values can be achieved through Eq. (1):

$$EE = \frac{C_D}{C_O} \times 100\% \quad (1)$$

in which C_O is a theoretical value according to the preparation conditions using Eq. (2):

$$C_O\% = \frac{f_1 * C_{helicid}}{f_1 * \left(C_{helicid} + C_{PVP1}\right) + f_2 * \left(C_{sucralose} + C_{PVP2}\right) + f_3 * \left(C_{SDS} + C_{PVP3}\right)} \quad (2)$$

where f and C denote fluid flow rate and solute concentration, respectively; the subscript "1,","2," and "3″ refer to the fluid number, respectively.

2.4.2 Fast disintegrating observations

In vitro dissolution and additional two self-created methods were explored to observe the fast disintegrating and fast-dissolving processes of the prepared TJNs. Those TJNs prepared during the optimization processes (i.e., containing blue and red markers) were exploited for distinguishing the sequential dissolution of encapsulated functional ingredients.

2.4.3 In vitro dissolution tests

In vitro dissolution tests were conducted according to the paddle method in Chinese Pharmacopoeia (2020 Ed.). An amount of 100.0 mg TJNs were immersed in 600 mL normal saline at 35 ± 0.5 °C. At predetermined time points, 5.0 mL aliquot was withdrawn, and 5.0 mL of fresh saline was added. The amounts of helicide released were measured and calculated. Experiments were repeated 3 times.

3 Results and discussion

3.1 The new tri-fluid electrospinning process

Among the four parts of an electrospinning system, i.e., power supply, collector, syringe pump, and spinneret, the spinneret is the most innovative one [78–80]. Often, a new spinneret can determine a new electrospinning process, for example, an eccentric spinneret for a side-by-side electrospinning [81] and a concentric spinneret for a coaxial electrospinning [82, 83]. In this study, a new spinneret is developed, whose information is concluded in Fig. 1. Figure 1a is a whole digital view of the spinneret, which has a weight of 37.2 g for easily installing the electrospinning system. Figure 1b shows the co-outlets of nozzle, with two outlets in a typical round shape and the third outlet in a "strange arch" shape. The inner arrangement of the metal capillaries and the combinations are disclosed in Fig. 1c. In the "strange arch" shape, a large contact surface area between the three working fluids can be ensured during the working processes for a successful preparation (as indicated by the letter "A"). The spinneret is very convenient for being fixed by one syringe pump, which the syringe holding the fluid passing through the "strange arch shape" can be directly inserted into the spinneret; the other two working fluids can be guided to the spinneret through the high elastic silicon tubes, as shown by the digital picture of Fig. 1d.

Helicide is not soluble in water and ethanol but soluble in DMAc. SDS is soluble in water. Thus, although PVP is soluble in water and almost all the organic solvents, it is impossible for blending all the functional ingredients, helicide, SDS, and sucralose, with PVP to form a co-dissolving solution, and thus it is impossible to prepare a multiple-component nanocomposite using a single-fluid blending process. Multiple-fluid electrospinning has the capability of encapsulating multiple components from different working fluids. Here, to investigate the tri-fluid working process through the structural spinneret, color markers methylene blue and basic fuchsin were loaded into the co-dissolved working fluids of helicide-PVP K60 and sucralose-PVP K10, respectively. Only the fluid containing PVP K60 and SDS was transparent. The arrangements of three pumps for constructing the home-made electrospinning apparatus are shown in Fig. 2a. After optimizing the fluid flow rates of three working fluids, a droplet dripped from outlet of the spinneret's nozzle can be observed in the up-right inset of Fig. 2a, showing the co-pumped out three fluids before applying the high voltage for preparing TJNs. The ways that the three working fluids were guided into the spinneret and the connection between the power supply and the spinneret through an alligator clip are shown in the digital photo of Fig. 2b. When the applied

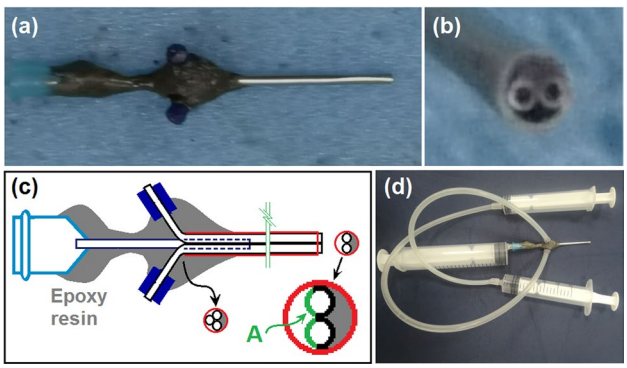

Fig. 1 Construction of the structural spinneret: **a** a whole digital view; **b** the co-outlets of nozzle (the other "arch" was blocked by epoxy resin); **c** a diagram showing the inner arrangement of the metal capillaries and their combination using epoxy resin; **d** a digital picture telling the connections of spinneret with the three syringes holding the three sorts of working fluids

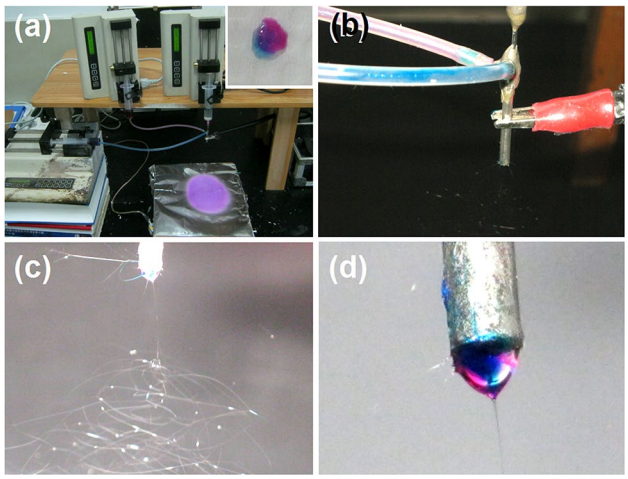

Fig. 2 Implementation of the tri-fluid electrospinning processes: **a** a digital image of the home-made electrospinning apparatus, the up-right inset shows a droplet from the nozzle of spinneret before applying the high voltage; **b** the ways that the three working fluids were led into the spinneret and the connection between the power supply and the spinneret through an alligator clip; **c** a typical working process with bending and whipping loops; **d** a typical compound Taylor cone with color markers

voltage was lifted to 15 kV, the electrospinning process is stable. A typical working process was observed in Fig. 2c. The platitudes are a compound Taylor cone, followed by a straight fluid line and an instable region, characterized by the gradually enlarged bending and whipping circles. An enlarged image of the compound Taylor cone is given in Fig. 2d. The two colors (blue and red) and a transparent section in the cone demonstrated the co-electrospinning of the three working fluids.

As mentioned previously, the publications about coaxial electrospinning and core-sheath nanofibers are greatly larger than their counterparts, i.e., side-by-side electrospinning and Janus nanofibers. Similarly, the investigations about tri-axial electrospinning and tri-layer core-sheath nanofibers are reported in decades of papers, but few articles can be found about the tri-fluid side-by-side electrospinning and tri-layer Janus nanofibers. The key difficult point is that it is very hard to keep the side-by-side working fluids to be drawn in an integrated manner through the Taylor cone, straight fluid jet, and bending and whipping processes [84, 85]. When these fluids are pumped out from the nozzles, they carry the same electrical charges and thus it is inevitable to repel each other using a traditional spinneret comprising three parallel metal capillaries (diagrammed in Fig. 3). Particularly, the charges distribute in an irregular format. These adverse factors would make the formation of integrated TJNs failure due to separation of each sections during the electrospinning processes.

In obvious contrast, the present new spinneret has its advantages to ensure a robust and effective preparation of TJNs. First of all, the three fluids have a larger contact surface area (as indicated by "A" in Fig. 1). Second, the working fluids can be more easily self-regulated into a round shape due to surface tension although an irregular shape of the outlet of nozzle (as indicated by letter "A" in Fig. 3). Third, the spinneret is coated mostly by epoxy resin, leaving only a small section of metal capillary for connecting the alligator clip, which is favorite for an effective transferring of the electrical energy to the working fluid, other than being scattering to the environment [86].

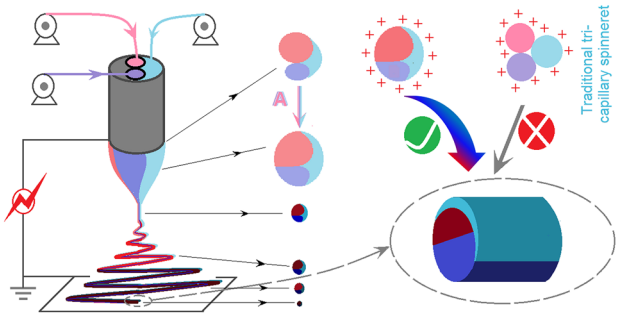

Fig. 3 The formation mechanism of the electrospun TJNs using the new spinneret

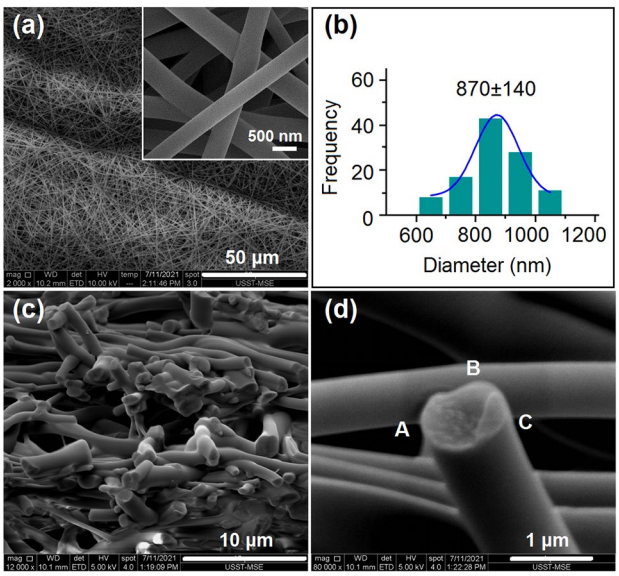

Fig. 4 Morphologies of the prepared tri-section Janus nanohybrids: **a** the surface morphology of the nanofibers, the up-right inset shows an enlarged image; **b** the nanofibers' diameters and their size distribution; **c** the cross-sections of the tri-section nanofibers; **d** a typical image of the nanofiber's cross-section, in which, "A"(sucralose-PVP 10), "B"(helicide-PVP K60), "C" (SDS-PVP K60), three different sections can be clearly discerned

3.2 The TJNs' morphologies and inner structures

The surface morphologies of the electrospun TJNs are shown in Fig. 4a, with an enlarge image in its up-right inset. The estimated diameters of these nanofibers are about 870 ± 140 nm (Fig. 4b). Clearly, there TJNs are round and in a straight line format with smooth surface. Although unspinnable fluid of PVP K10-sucralose was exploited, the electrospinnable PVP K60-helicide and PVP K60-SDS fluids were able to ensure the formation of linear nanofibers without beads or spindles. The cross-sections of TJNs are shown in Fig. 4c and d. It is obvious that three different sections (labeled with "A," "B," "C" beside) within the cross-section of nanofiber can be discerned.

TEM images of the TJNs are shown in Fig. 5a to c. The gray levels in the TEM images taken under bright field are often from three aspects, i.e., element, thickness, and density. When the magnification is 5,000, all the nanofibers showed the same gray levels, which is shown in Fig. 5a. However, when the magnification is enlarged to 200,000, the different gray levels within the TJNs can be clearly distinguished out, as exhibited in Fig. 5b and c. The multiple gray levels should have a close relationship with the view angle on the nanofibers. A diagram showing the formations of different regions with various gray levels is drawn in Fig. 5d. The thicker and the more sections involved, the darker the gray level is.

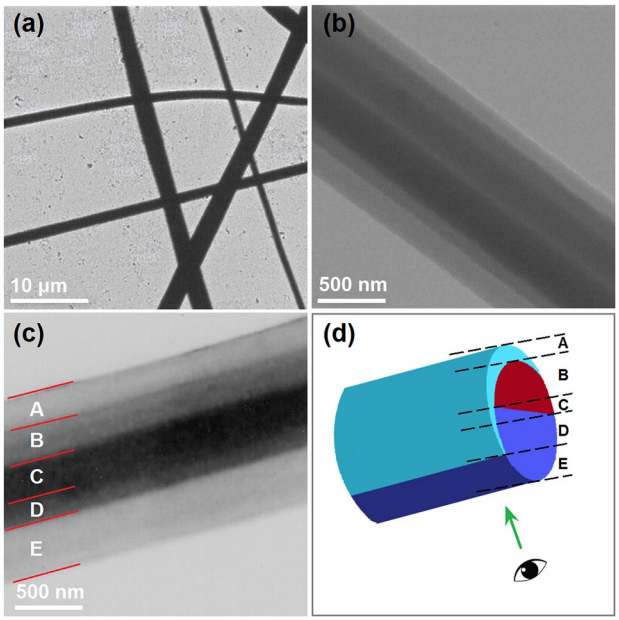

Fig. 5 Inner structures of the prepared TJNs: **a** a whole TEM image of the nanofibers on the carbon membrane; **b** and **c** two typical TEM images; **d** a diagram showing the formations of different regions with various gray levels

3.3 The three sections of polymer-based nanocomposites within the TJNs

Essentially, electrospinning is a physical method, which electrostatic energy is exploited to eliminate the solvents from the working fluids at an extremely short time period, often at a scale of several decades of milliseconds [87–89]. Based on this situation, it is often anticipated that the physical state of components in the liquid working fluids will be propagated into the solid nanofibers. This advantage makes electrospinning a highly popular tool for preparing drug-polymer composites or molecular solid dispersion in pharmaceutical field [34, 90, 91]. Thus, there are numerous nanofiber-based composites or solid dispersion in literature, which are often fabricated using a single-fluid blending electrospinning process [20, 92, 93]. The active ingredient, the filament-forming polymer, and sometimes other additives are all co-dissolved into one electrospinnable working fluid, and then the fluid was transferred into polymer-based composites.

However, these homogeneous polymer-based composites and also the single-fluid blending electrospinning are only limited to some special situations, in which the drug, the polymer, and also the additive can be co-dissolved together in a solvent or a solvent mixture. Meanwhile, the single solvent system must ensure that the polymer has fine electrospinnability and must ensure that the drug and additives have enough loading for functional performances. Thus, multiple-fluid electrospinning processes and the related complex nanostructures are able to expand the capability of electrospinning in generating functional nanomaterials. Here, the tri-fluid side-by-side electrospinning processes have exploited three different kinds

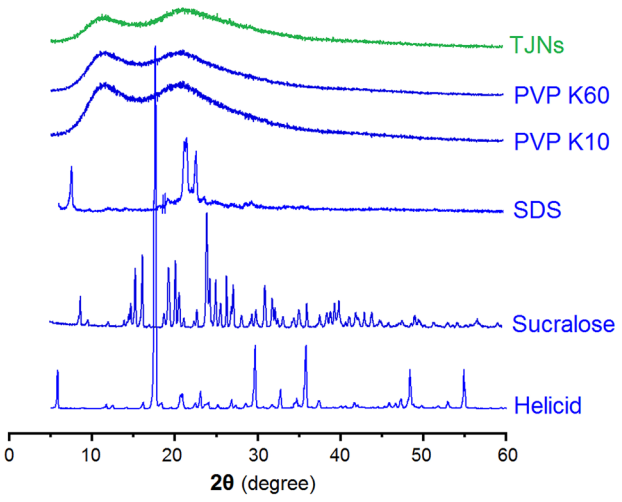

Fig. 6 XRD patterns of the tri-section TJNs and the five raw materials including PVP K60 and K10, SDS, sucralose, and helicide

of solvent systems, i.e., ethanol and DMAc for PVP K60 and helicide, ethanol for PVP K30 and sucralose, and ethanol and water for PVP K60 and SDS. All the solutions were transparent liquids. After electrospinning, the TJNs' XRD patterns were achieved (Fig. 6). Compared with the XRD patterns of the raw helicide, sucralose, and SDS, in which Bragg sharp peaks suggesting crystalline materials, there are no any sharp peaks on the curve of TJNs, but two halos like the XRD patterns of PVP K10 and K60. These phenomena gives a hint that all the crystalline helicide, SDS, and sucralose have been transferred into amorphous polymer-based composites in their owns' sections of tri-section Janus products, whereas the whole TJNs are nanohybrids, which consist of three different sorts of polymer-based nanocomposites.

In this study, three different functional ingredients were successfully encapsulated into two different polymeric matrices to create the designed TJNs. Their molecular formula are concluded in Fig. 7. Although the polymer matrices PVP K10 and K60 have their differences in molecular weights and dissolution rates, they similarly have numerous C = O groups in their molecules and meanwhile the N bring some positive charges. Both helicide and sucralose have OH groups in their molecules. Thus, it can be anticipated that both of them have fine compatibility with PVP. This is because the favorite secondary interaction, i.e., hydrogen bonding, can be formed between them, which can keep a high stability of the composites through a long time period [11]. SDS, as a transmembrane enhancer, has negative charges on the element O; thus, electrostatic actions can form between SDS and PVP, i.e., PVP-SDS nanocomposites also have a high stability. Thus, it is no strange that all the sharp peaks presented in the figure regions of the ATR-FTIR spectra of sucralose, SDS, and helicide have disappeared in the spectra of TJNs due to the secondary interactions, which have revised their covalent bonds' original stretching and bending actions. Meanwhile, compared with the spectra of PVP K10 and K60, the characteristic peak places of C = O of TJNs have showed some red shifts from 1662 to 1657 cm^{-1}.

3.4 The functional performances of the prepared TJNs

The measured content of helicide in the TJNs was 8.23 ± 0.41%. According to the experimental conditions, the theoretical concentration is 8.12%. Thus, the drug loading efficiency is 101.4%. This result suggests that there were no any drug losing during the electrospinning process. All the drugs have been encapsulated into the TJNs due to just a fast drying procedure of the co-dissolving solutions, which is similar as all the other electrospinning processes.

Three different methods are developed for measuring the fast dissolution properties of the electrospun TJNs and disclosing the sequential release performances. Shown in Fig. 8, a disintegration experiment was carried out using a piece of glass slide. After about 10 min of the depositions of TJNs, a drop of water was dripped on the TJNs. A camera was exploited to record the fast disintegrating process. After contacting the water, the TJNs were quickly disintegrated into transparent gels, as demonstrated by the gradually enlarged circle from 1 to 6 in Fig. 8. The total time was 4 s for the buried characters "USST" (abbreviation of

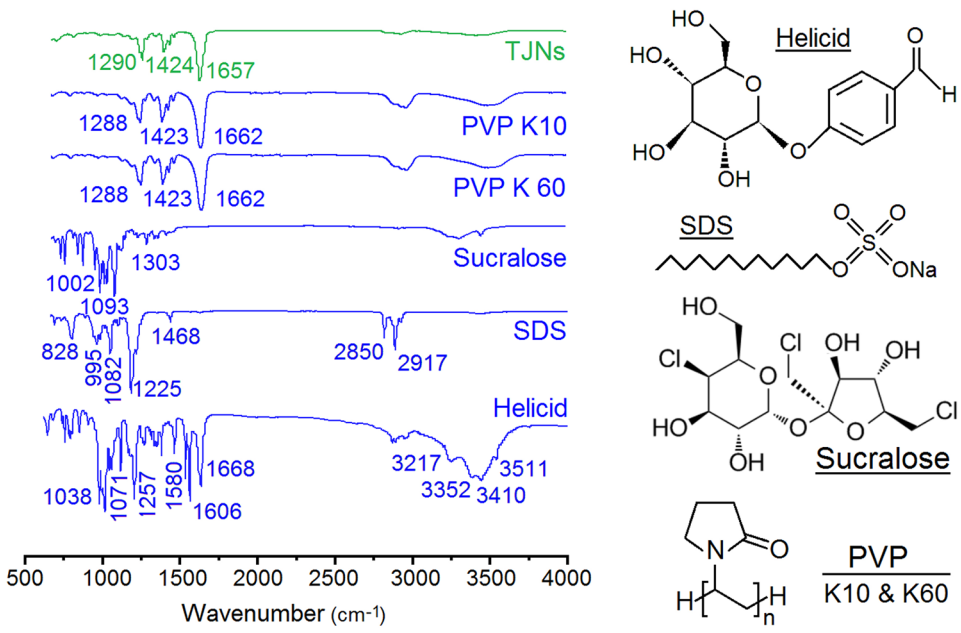

Fig. 7 ATR-FTIR spectra of the TJNs and the five raw materials including PVP K60 and K10, SDS, sucralose, and helicide, and their molecular formula

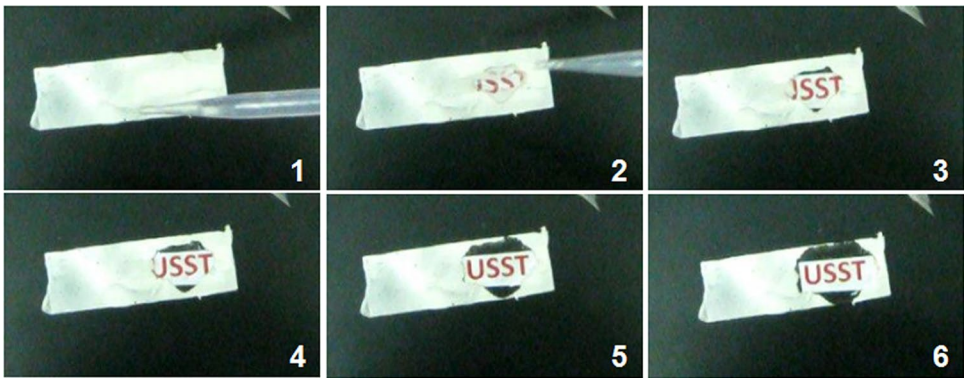

Fig. 8 A glass slide was used to collect TJNs to test the fast disintegrating processes, the time cost from 1 to 6 was 4 s

University of Shanghai for Science and Technology) to be completely appeared.

For drug delivery, the drug release is most frequently measured using the quantitative methods, particularly those dosages form for drug sustained release [22]. The above-mentioned fast disintegrating experiment was just a qualitative observation. According to Chinese Pharmacopoeia (2020 Ed.), the paddle method was used to measure the dissolution of helicide. As the SDS and sucralose have no any absorbance at the maximum wavelength of $\lambda_{max} = 270$ for helicide. Thus, the absorbance of dissolution media were detected, and the values were exploited to calculate the drug concentration using the standard equation. The result is shown in Fig. 9. As anticipated, all the loaded helicide in the TJNs was freed within 1 min. In comparison, the helicide powders ($\leq$ 50 μm) released only 3.6 ± 1.4% into the dissolution media after a time period of 30 min, suggesting a typical poorly water-soluble drug.

The TJNs prepared during the optimization of experimental parameters (i.e., with color markers) were exploited to distinguish the dissolution procedures of different functional

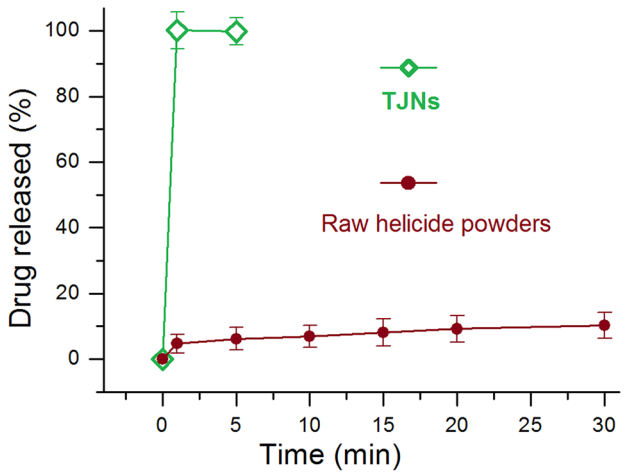

Fig. 9 The in vitro dissolution test results of the TJNs and raw helicide powders

ingredients encapsulated in the TJNs. Shown in Fig. 10, a piece of TJNs were placed on a cup of water with a stirring rate of 50 rpm. The whole time from 1 to 6 was 34 s. During the processes, two phenomena were clear, one is that the center of the floated solid TJNs (in the shape of "T" due to the stirring) was mainly in purple and blue colors, whereas the dissolution medium was in pink color, suggesting that the red marker dissolved and diffused to the dissolution media faster than the blue marker. Both of the red and blue markers have fine water solubility, and both of them contacted the environments due to the Janus structures. Thus, it is the solubility differences of their polymeric matrices, i.e., PVP K10 and PVP K60, that made the two colors be released through different rates through the polymeric erosion mechanisms. The other is that the water gradually turned its color from pink to purple, also suggested that the later dissolution and diffusion of blue marker. These phenomena suggest that the sucralose loaded with PVP K10 will be faster released than the drug helicide encapsulated with PVP K60. Thus, in the administration applications, the sweet taste of sucralose will be firstly felt by the patients and will mask the bitterness of helicide, and thus the patients' compliance can be effectively improved by this sequential release performance.

Helicide is a monomer extracted from the fruit of wild plant radish tree of *Longan* family [94]. It is frequently used for neurasthenia, neurasthenia syndrome, and vascular nerve headache. However, its poor water solubility has greatly limited its applications, and its bitter taste has decreased its patient compliance [95]. Here, it was selected as a model active pharmaceutical ingredient to develop a nanofiber-based DDS. It is expected that the suggested protocols can be applied to many other drugs due to the strategies and mechanisms disclosed here. Shown in the diagram of Fig. 11, the TJNs have three sections in an irregular side-by-side manner. All the three sections contact the environments. The side from the "arch shape" outlet of spinneret has the thinnest thickness and largest surface, which can also play a role in making a different dissolution rate besides the polymeric matrices, although this point cannot be detected presently due to the extremely fast whole dissolution rate.

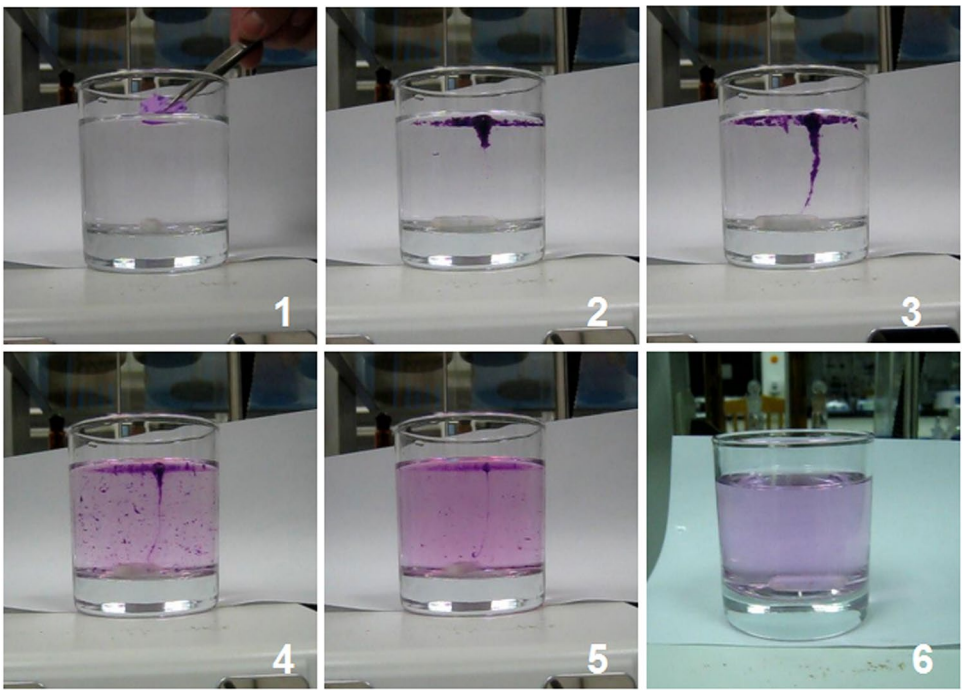

Fig. 10 A disintegrating release experiment for measuring the dissolution procedure of functional ingredients within the TJNs by using the color markers

The release of SDS in an earlier step can benefit an effective trans membrane of the later released drug molecules. Meanwhile, the release of sucralose will be rapider than the helicide for a better compliance, as detected in the above-mentioned experiments. Thus, the whole sequential release of SDS, sucralose, and helicide from their owns' PVP-based nanocomposites will ensure the tri-section Janus medicated hybrids an ideal nano DDS for the patients.

In the traditional electrospun fast disintegrating membranes, orodispersible films, and sublingual membranes, the drug and also the additive are simultaneously dissolved [47]. Here, the TJNs not only release the loaded functional ingredients in an immediate manner, but during the fast process, the release of different ingredients can be manipulated in a certain order. For drug delivery applications, this is favorite for the patients; the formerly release of sweeter and trans-membrane enhancer can effectively cover up the bite taste of drug and promote drug transportation to penetrate the biological mucosa due to an earlier release than drug and thus increase the conveniences, compliance, and effectiveness of drug delivery to the patients. This strategy, on one hand, should be not only useful for the delivery of a certain drug but should be more useful for manipulating the combined therapy of several different kinds of drugs, which are presently under investigations. On the other hand, with the hints from literature [96–98]. The protocols can be explored for developing a series of multifunctional hybrid and composite materials in other scientific fields such as food and agroforestry.

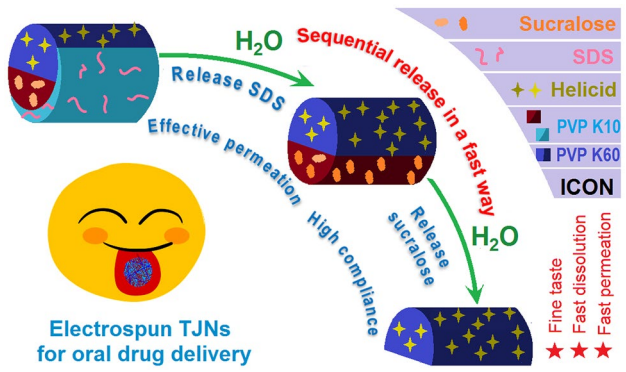

Fig. 11 Sequential release of sucralose, SDS, and helicide from the prepared TJNs

4 Conclusions

A new tri-fluid electrospinning, characterized by a home-made spinneret, was successfully developed for preparing tri-section Janus nano structures. Three functional ingredients, sucralose, SDS, and helicide were loaded separated into the Janus structures with two different polymeric matrices, i.e., PVP K10 and PVP K60. The prepared TJNs were demonstrated to have a linear morphology and comprise three nanocomposites, i.e., helicide-PVP K60, SDS-PVP K60, and sucralose-PVP K10, which are demonstrated by SEM and TEM images. XRD and ATR-FTIR verified that the functional ingredients, helicide, SDS, and sucralose, existed in their own sections in an amorphous state due to the favorite secondary interactions with the PVP matrices.

Two disintegrating experiments (with a drop of water and a cup of water) and in vitro dissolution tests demonstrate that the TJNs have the fast dissolution performances, and meanwhile, they can manipulate the sucralose, SDS, and helicide to be released in a sequential manner. This is useful for compliance (sweeter masking the bite taste of helicide) and effective (SDS as trans-membrane enhancer) drug delivery. The tri-fluid electrospinning and the TJNs reported here pave a new way for developing multiple functional nanomaterials.

Funding This study is financially supported by the Shanghai Natural Science Foundation (No.20ZR1439000) and the USST-NMU-Pengting Medical Corporation joint medical project (No. 20210937).

Declarations

Conflict of interest The authors declare no competing interests.

References

1. Mehta P, Rasekh M, Patel M, Onaiwu E, Nazari K, Kucuk I, Wilson PB, Arshad MS, Ahmad Z, Chang MW (2021) Recent applications of electrical, centrifugal, and pressurised emerging technologies for fibrous structure engineering in drug delivery, regenerative medicine and theranostics. Adv Drug Deliver Rev 175(8):113823. https://doi.org/10.1016/j.addr.2021.05.033
2. Chi ZM, Zhao SQ, Feng YX, Yang L (2020) On-line dissolution analysis of multiple drugs encapsulated in electrospun nanofibers. Int J Pharm 588(10):119800. https://doi.org/10.1016/j.ijpharm.2020.119800
3. Sa'adon S, Ansari MNM, Razak SIA, Anand JS, Nayan NHM, Ismail AE, Khan MUA, Haider A (2021) Preparation and physicochemical characterization of a diclofenac sodium-dual layer polyvinyl alcohol patch. Polymers 13(15):2459. https://doi.org/10.3390/polym13152459
4. Yu DG (2021) Preface-bettering drug delivery knowledge from pharmaceutical techniques and excipients. Curr Drug Deliv 18:2–3
5. Zhang Y, Li S, Xu Y, Shi X, Zhang M, Huang Y, Liang Y, Chen Y, Ji W, Kim JR, Song W, Yu DG, Kim I (2022) Engineering of hollow polymeric nanosphere-supported imidazolium-based ionic liquids with enhanced antimicrobial Activities. Nano Res. https://doi.org/10.1007/s12274-022-4160-6
6. Mouro C, Fangueiro R, Gouveia IC (2020) Preparation and characterization of electrospun double-layered nanocomposites membranes as a carrier for centella asiatica (L.). Polymers 12(11):2653. https://doi.org/10.3390/polym12112653
7. Saraogi GK, Tholiya S, Mishra Y, Mishra V, Albuttim A, Nayak P, Tambuwala MM (2022) Formulation development and evaluation of pravastatin-loaded nanogel for hyperlipidemia management. Gels 8(2):81. https://doi.org/10.3390/gels8020081
8. Bagliotti MA, Miguel SR, Chaves DSMP, Perosa FR, Gomes DOA, Marlus C (2021) Cellulose nanofibers improve the performance of retrograded starch/pectin microparticles for colon-specific delivery of 5-ASA. Pharmaceutics 13(9):1515. https://doi.org/10.3390/pharmaceutics13091515
9. Hou Z, Itagaki N, Kobayashi H, Tanaka K, Takarada W, Kikutani T, Takasaki M (2021) Bamboo charcoal/poly(l-lactide) fiber webs prepared using laser-heated melt electrospinning. Polymers 13(16):2776. https://doi.org/10.3390/polym13162776
10. Cervantes MYG, Kim J, Chitara B, Wymer N, Yan F (2021) N-halamine-decorated electrospun polyacrylonitrile nanofibrous membranes: characterization and antimicrobial properties. React Funct Polym 168:105058. https://doi.org/10.1016/j.reactfunctpolym.2021.105058
11. Bhusnure OG, Gholve SB, Giram PS, Gaikwad AV, Udumansha U, Mani G, Tae JH (2021) Novel 5-flurouracil-embedded nonwoven PVA - PVP electrospun nanofibers with enhanced anticancer efficacy: formulation, evaluation and in vitro anti-cancer activit. J Drug Deliv Sci Technol 64(8):102654. https://doi.org/10.1016/j.jddst.2021.102654
12. Li X, Chen K, Ji X, Yuan X, Lei Z, Ullah MW, Xiao J, Yang G (2021) Microencapsulation of poorly water-soluble finasteride in polyvinyl alcohol/chitosan microspheres as a long-term sustained release system for potential embolization applications. Eng Sci 13:106–120. https://doi.org/10.30919/es8d1159
13. Mehdi M, Hussain S, Gao BB, Shah KA, Mahar FK, Yousif M, Hussain S, Ahmed F (2021) Fabrication and characterization of rizatriptan loaded pullulan nanofibers as oral fast-dissolving drug system. Mater Res Express 8(5):055404. https://doi.org/10.1088/2053-1591/abff0b
14. Ding CB, Zhou CX, Fan YY, Liu Q, Zhang HF, Wu ZW (2022) Electrospun polylactic acid/sulfadiazine sodium/proteinase nanofibers and their applications in treating frostbite. J Appl Polym Sci 139(9):e51716. https://doi.org/10.1002/app.51716
15. Yu DG, Lv H (2022) Preface-striding into nano drug delivery. Curr Drug Deliv 19(1):2–4
16. Salim SA, Kamoun EA, Evans S, El-Moslamy SH, El-Fakharany EM, Elmazar MM, Abdel-Aziz AF, Abou-Saleh RH, Salaheldin TA (2021) Mercaptopurine-loaded sandwiched tri-layered composed of electrospun polycaprolactone/poly(methyl methacrylate) nanofibrous scaffolds as anticancer carrier with antimicrobial and antibiotic features: sandwich configuration nanofibers, release study and in vitro bioevaluation tests. Int J Nanomedicine 16:6937–6955. https://doi.org/10.2147/IJN.S332920
17. Balusamy B, Celebioglu A, Senthamizhan A, Uyar T (2020) Progress in the design and development of "fast-dissolving" electrospun nanofibers based drug delivery systems - a systematic review. J Control Release 326:482–509. https://doi.org/10.1016/j.jconrel.2020.07.038
18. Manakhov AM, Sitnikova NA, Tsygankova AR, Alekseev AY, Adamenko LS, Permyakova E, Baidyshev VS, Popov ZI, Blahová L, Eliáš M, Zajíčková L, Solovieva AO (2021) Electrospun biodegradable nanofibers coated homogenously by Cu magnetron sputtering exhibit fast ion release Computational and experimental study. Membranes 11(12):965. https://doi.org/10.3390/membranes11120965
19. Vineis C, Maya IC, Mowafi S, Varesano A, Ramírez DOS, Taleb MA, Tonetti C, Guarino V, El-Sayed H (2021) Synergistic effect of sericin and keratin in gelatin based nanofibers for in vitro applications. Int J Biol Macromol 190(11):375–381. https://doi.org/10.1016/j.ijbiomac.2021.09.007
20. Miranda CS, Silva AFG, Pereira-Lima SMMA, Costa SPG, Homem NC, Felgueiras HP (2022) Tunable spun fiber constructs in biomedicine: influence of processing parameters in the fibers' architecture. Pharmaceutics 14(1):164. https://doi.org/10.3390/pharmaceutics14010164
21. Mary AS, Raghavan VS, Kagula S, Krishnakumar V, Kannan M, Gorthi SS, Rajaram K (2021) Enhanced in vitro wound healing using PVA/B-PEI nanofiber mats: a promising wound therapeutic agent against ESKAPE and opportunistic pathogens. ACS Appl Bio Mater 4(12):8466–8476. https://doi.org/10.1021/acsabm.1c00985
22. Mirzaie Z, Reisi-Vanani A, Barati M, Atyabi SM (2021) The drug release kinetics and anticancer activity of the GO/PVA-curcumin nanostructures: the effects of the preparation method and the GO amount. J Pharm Sci 110(11):3715–3725. https://doi.org/10.1016/j.xphs.2021.07.016

23. Haidar MK, Timur SS, Demirbolat GM, Nemutlu E, Gürsoy RN, Ulubayram K, Öner L, Eroğlu H (2021) Electrospun nanofibers for dual and local delivery of neuroprotective drugs. Fiber Polym 22(2):334–344. https://doi.org/10.1007/s12221-021-0228-2
24. Peres RM, Sousa JML, Oliveira MOD, Rossi MV, Oliveira RRD, Lima NBD, Bernussi A, Warzywoda J, Sarmento B, Munahoz AH (2021) Pseudoboehmite as a drug delivery system for acyclovir. Sci Rep 11(1):15448. https://doi.org/10.1038/s41598-021-94325-y
25. Ghosal K, Augustine R, Zaszczynska A, Barman M, Jain A, Hasan A, Kalarikkal N, Sajkiewicz P, Thomas S (2021) Novel drug delivery systems based on triaxial electrospinning based nanofibers. React Funct Polym 163:104895. https://doi.org/10.1016/j.reactfunctpolym.2021.104895
26. Tubtimsri S, Weerapol Y (2021) Improvement in solubility and absorption of nifedipine using solid solution: correlations between surface free energy and drug dissolution. Polymers 13(17):2963. https://doi.org/10.3390/polym13172963
27. Kiss K, Hegedüs K, Vass P, Vári-Mező D, Farkas A, Nagy ZK, Molnár L, Tóvári J, Mező G, Marosi G (2021) Development of fast-dissolving dosage forms of curcuminoids by electrospinning for potential tumor therapy application. Int J Pharm 611(2):121327. https://doi.org/10.1016/j.ijpharm.2021.121327
28. Łyszczarz E, Brniak W, Szafraniec-Szczęsny J, Majka TM, Majda D, Zych M, Pielichowski K, Jachowicz R (2021) The impact of the preparation method on the properties of orodispersible films with aripiprazole: electrospinning vs. casting and 3D printing methods. Pharmaceutics 13(8):1122. https://doi.org/10.3390/pharmaceutics13081122
29. Xu G, Chen X, Zhu Z, Wu P, Wang H, Chen X, Gao W, Liu Z (2020) Pulse gas-assisted multi-needle electrospinning of nanofibers. Adv Compos Hybrid Mater 3(1):98–113. https://doi.org/10.1007/s42114-019-00129-0
30. Ziyadi H, Baghali M, Bagherianfar M, Mehrali F, Faridi-Majidi R (2021) An investigation of factors affecting the electrospinning of poly (vinyl alcohol)/kefiran composite nanofibers. Adv Compos Hybrid Mater 4:1–12. https://doi.org/10.1007/s42114-021-00230-3
31. Liu Y, Chen X, Liu Y, Gao Y, Liu P (2022) Electrospun coaxial fibers to optimize the release of poorly water-soluble drug. Polymers 2022(14):469. https://doi.org/10.3390/polym14030469
32. Kyselica R, Enikov ET, Anton R (2021) Method for production of aligned nanofibers and fiber elasticity measurement. J Mech Behav Biomed 113(1):104151. https://doi.org/10.1016/j.jmbbm.2020.104151
33. Zare M, Dziemidowicz K, Williams GR, Ramakrishna S (2021) Encapsulation of pharmaceutical and nutraceutical active ingredients using electrospinning processes. Nanomaterials 11(8):1968. https://doi.org/10.3390/nano11081968
34. Kalous T, Holec P, Erben J, Bilek M, Batka O, Pokorny P, Chaloupek J, Chvojka J (2021) The optimization of alternating current electrospun PA 6 solutions using a visual analysis system. Polymers 13(13):2098. https://doi.org/10.3390/polym13132098
35. ljohani MA, Alkabli J, Abualnaja MM, Alrefaei AF, Almehmadi SJ, Mahmoud MHH, El-Metwaly NM (2021) Electrospun AgNPs-polylactate nanofibers and their antimicrobial applications. React Funct Polym 167:104999. https://doi.org/10.1016/j.reactfunctpolym.2021.104999
36. Görgün N, Özer Ç, Polat K (2019) A new catalyst material from electrospun PVDF-HFP nanofibers by using magnetron-sputter coating for the treatment of dye-polluted waters. Adv Compos Hybrid Mater 2(3):423–430. https://doi.org/10.1007/s42114-019-00105-8
37. Panthi G, Ranjit R, Khadka S, Gyawali KR, Kim H-Y, Park M (2020) Characterization and antibacterial activity of rice grain-shaped ZnS nanoparticles immobilized inside the polymer electrospun nanofibers. Adv Compos Hybrid Mater 3(1):8–15. https://doi.org/10.1007/s42114-020-00141-9
38. Deng L, Zhang H (2020) Recent advances in probiotics encapsulation by electrospinning. ES Food Agrofor 2:3–12. https://doi.org/10.30919/esfaf1120
39. Gao C, Deng W, Pan F, Feng X, Li Y (2020) Superhydrophobic electrospun PVDF membranes with silanization and fluorosilanization co-functionalized CNTs for improved direct contact membrane distillation. Eng Sci 9:35–43. https://doi.org/10.30919/es8d905
40. Wu F, He P, Chang X, Jiao W, Liu L, Si Y, Yu J, Ding B (2021) Visible-light-driven and self-hydrogen-donated nanofibers enable rapid-deployable antimicrobial bioprotection. Small 17(12):2100139. https://doi.org/10.1002/smll.202100139
41. Zhang L, Li LF, Wang LC, Nie J, Ma GP (2020) Multilayer electrospun nanofibrous membranes with antibacterial property for air filtration. Appl Surf Sci 515(6):145962. https://doi.org/10.1016/j.apsusc.2020.145962
42. Hsiung E, Celebioglu A, Chowdhury R, Kilic ME, Durgun E, Altier C, Uyar T (2022) Antibacterial nanofibers of pullulan/tetracycline-cyclodextrin inclusion complexes for fast-disintegrating oral drug delivery. J Colloid Interf Sci 610:321–333. https://doi.org/10.1016/j.jcis.2021.12.013
43. McKee MG, Layman JM, Cashion MP, Long TE (2006) Phospholipid nonwoven electrospun membranes. Science 311(5759):353–355. https://doi.org/10.1126/science.1119790
44. Song Y, Huang H, He D, Yang M, Wang H, Zhang H, Li J, Li Y, Wang C (2021) Gallic acid/2-hydroxypropyl-β-cyclodextrin inclusion complexes electrospun nanofibrous webs: fast dissolution, improved aqueous solubility and antioxidant property of gallic acid. Chem Res Chinese Universities 37(3):450–455. https://doi.org/10.1007/s40242-021-0014-0
45. Habibi N, Kamaly N, Memic A, Shafiee H (2016) Self-assembled peptide-based nanostructures: smart nanomaterials toward targeted drug delivery. Nano Today 11(1):41–60. https://doi.org/10.1016/j.nantod.2016.02.004
46. Isaacoff BP, Brown KA (2017) Progress in top-down control of bottom-up assembly. Nano Lett 17(11):6508–6510. https://doi.org/10.1021/acs.nanolett.7b04479
47. Ning T, Zhou Y, Xu H, Guo S, Wang K, Yu DG (2021) Orodispersible membranes from a modified coaxial electrospinning for fast dissolution of diclofenac sodium. Membranes 11(11):802. https://doi.org/10.3390/membranes11110802
48. Lv H, Guo S, Zhang G, He W, Wu Y, Yu DG (2021) Electrospun structural hybrids of acyclovir-polyacrylonitrile at acyclovir for modifying drug release. Polymers 13:4286. https://doi.org/10.3390/polym13244286
49. Zhou K, Wang M, Zhou Y, Sun M, Xie Y, Yu DG (2022) Comparisons of antibacterial performances between electrospun polymer@drug nanohybrids with drug-polymer nanocomposites. Adv Compos Hybrid Mater. https://doi.org/10.1007/s42114-021-00389-9
50. He H, Wu M, Zhu J, Yang Y, Ge R, Yu DG (2021) Engineered spindles of little molecules around electrospun nanofibers for biphasic drug release. Adv Fiber Mater. https://doi.org/10.1007/s42765-021-00112-9
51. Zhang X, Guo S, Qin Y, Li C (2021) Functional electrospun nanocomposites for efficient oxygen reduction reaction. Chem Res Chinese Universities 37(3):379–393. https://doi.org/10.1007/s40242-021-1123-5
52. Yang S, Liu Y, Jiang Z, Gu J, Zhang D (2018) Thermal and mechanical performance of electrospun chitosan/poly(vinyl alcohol) nanofibers with graphene oxide. Adv Compos Hybrid Mater 1(4):722–730. https://doi.org/10.1007/s42114-018-0060-3
53. Yang P, Zhao H, Yang Y, Zhao P, Zhao X, Yang L (2020) Fabrication of N, P-codoped Mo_2C/carbon nanofibers via electrospinning

as electrocatalyst for hydrogen evolution reaction. ES Mater Manuf 7:34–39. https://doi.org/10.30919/esmm5f618
54. Xie W, Shi Y, Wang Y, Zheng Y, Liu H, Hu Q, Wei S, Gu H, Guo Z (2021) Electrospun iron/cobalt alloy nanoparticles on carbon nanofibers towards exhaustive electrocatalytic degradation of tetracycline in wastewater. Chem Eng J. https://doi.org/10.1016/j.cej.2020.126585
55. Wu C, Wei XH, Zhao K, Jiang JY, Jiao MZ, Cheng JH, Tang Z, Guo Z, Tang YF (2021) Novel dam-like effect based on piezoelectric energy conversion for drug sustained release of drug-loaded TiO_2@$BaTiO_3$ coaxial nanotube coating. Ceram Int 47(12):17550–17559. https://doi.org/10.1016/j.ceramint.2021.03.073
56. Darbasizadeh B, Mortazavi SA, Kobarfard F, Jaafari MR, Hashemi A, Farhadnejad H, Feyzi-barnaji B (2021) Electrospun doxorubicin-loaded PEO/PCL core/sheath nanofibers for chemopreventive action against breast cancer cells. J Drug Deliv Sci Technol 64(8):102576. https://doi.org/10.1016/j.jddst.2021.102576
57. Kazsoki A, Palcsó B, Alpár A, Snoeck R, Andrei G, Zelkó R (2022) Formulation of acyclovir (core)-dexpanthenol (sheath) nanofibrous patches for the treatment of herpes labialis. Int J Pharm 611:121354. https://doi.org/10.1016/j.ijpharm.2021.121354
58. Kumar D, Kumar S, Kumar S, Rohatgi S, Kundu PP (2021) Synthesis of rifaximin loaded chitosan-alginate core-shell nanoparticles (Rif@CS/Alg-NPs) for antibacterial applications. Int J Biol Macromol 183(7):962–971. https://doi.org/10.1016/j.ijbiomac.2021.05.022
59. Lv Y, Zhu L, Xu H, Yang L, Liu Z, Cheng D, Cao X, Yun J, Cao D (2019) Core/shell template-derived Co, N-doped carbon bifunctional electrocatalysts for rechargeable Zn-air battery. Eng Sci 7:26–37. https://doi.org/10.30919/es8d768
60. Xu X, Zhang M, Lv H, Yang Y, Yu DG (2022) Electrospun polyacrylonitrile-based lace nanostructures and their Cu(II) adsorption. Sep Purif Technol. https://doi.org/10.1016/j.seppur.2022.120643
61. Duan GG, Jin MD, Wang F, Greiner A, Agarwal S, Jiang SH (2021) Core effect on mechanical properties of one dimensional electrospun core-sheath composite fibers. Compos Comm 25:100773. https://doi.org/10.1016/j.coco.2021.100773
62. Liu Y, Chen X, Yu DG, Liu H, Liu Y, Liu P (2021) Electrospun PVP-core/PHBV-shell fibers to eliminate tailing off for an improved sustained release of curcumin. Mol Pharm 18(11):4170–4178. https://doi.org/10.1021/acs.molpharmaceut.1c00559
63. Sun Z, Zussman E, Yarin AL, Wendorff JH, Greiner A (2003) Compound core–shell polymer nanofibers by co-electrospinning. Adv Mater 15(22):1929–1932. https://doi.org/10.1002/adma.200305136
64. Dzenis Y (2004) Spinning continuous fibers for nanotechnology. Science 304(5679):1917–1919. https://doi.org/10.1126/science.1099074
65. Wei X, Chen L, Wang Y, Sun Y, Ma C, Yang X, Jiang S, Duan G (2022) An electrospinning anisotropic hydrogel with remotely-controlled photo-responsive deformation and long-range navigation for synergist actuation. Chem Eng J 433(3):134258. https://doi.org/10.1016/j.cej.2021.134258
66. Wang M, Hou J, Yu D-G, Li S, Zhu J, Chen Z (2020) Electrospun tri-layer nanodepots for sustained release of acyclovir. J Alloys Compd 846:156471. https://doi.org/10.1016/j.jallcom.2020.156471
67. Labbaf S, Ghanbar H, Stride E, Edirisinghe M (2014) Preparation of multilayered polymeric structures using a novel four-needle coaxial electrohydrodynamic device. Macromol Rapid Commun 35(6):618–623. https://doi.org/10.1002/marc.201300777
68. Zhang X, Chi C, Chen J, Zhang X, Gong M, Wang X, Xue J (2021) Electrospun quad-axial nanofibers for controlled and sustained drug delivery. Mater Des 206:109732. https://doi.org/10.1016/j.matdes.2021.109732
69. Zhao K, Lu Z-H, Zhao P, Kang S-X, Yang Y-Y, Yu D-G (2021) Modified tri–axial electrospun functional core–shell nanofibrous membranes for natural photodegradation of antibiotics. Chem Eng J 425:131455. https://doi.org/10.1016/j.cej.2021.131455
70. Gupta P, Wilkes GL (2003) Some investigations on the fiber formation by utilizing a side-by-side bicomponent electrospinning approach. Polymer 44(20):6353–6359. https://doi.org/10.1016/S0032-3861(03)00616-5
71. Liu YJ, Wang JL, Shao Y, Deng RH, Zhu JT, Yang ZZ (2022) Recent advances in scalable synthesis and performance of Janus polymer/inorganic nanocomposites. Prog Mater Sci 124(2):100888. https://doi.org/10.1016/j.pmatsci.2021.100888
72. Liu X, Xu H, Zhang M, Yu DG (2021) Electrospun medicated nanofibers for wound healing: review. Membranes 11(10):770. https://doi.org/10.3390/membranes11100770
73. Aidana Y, Wang Y, Li J, Chang S, Wang K, Yu D-G (2022) Fast dissolution electrospun medicated nanofibers for effective delivery of poorly water-soluble drugs. Curr Drug Deliv. https://doi.org/10.2174/1567201818666210215110359
74. Jiang SH, Chen YM, Duan GG, Mei CT, Greiner A, Agarwal S (2018) Electrospun nanofiber reinforced composites: a review. Polym Chem 9:2685–2720. https://doi.org/10.1039/c8py00378e
75. Xie YR, Ma QL, Qi HN, Liu XN, Chen XY, Jin Y, Li D, Yu WS, Dong XT (2021) A fluorescent triboelectric nanogenerator manufactured with a flexible Janus nanobelt array concurrently acting as a charge-generating layer and charge-trapping layer. Nanoscale 13(45):19144–19154. https://doi.org/10.1039/d1nr06533e
76. Qi HN, Wang GY, Ma QL, Li D, Dong XT, Yu WS, Wang JX, Liu GX, Zhang XJ (2022) Conjugative electrospinning towards Janus-type nanofibers array membrane concurrently displaying dual-functionality of improved red luminescence and tuneable superparamagnetism. J Mater Sci 10(2). https://doi.org/10.1007/s10854-021-07635-2
77. Zhang M, Song W, Tang Y, Xu X, Huang Y, Yu DG (2022) Polymer-based nanofiber-nanoparticle hybrids and their medical applications. Polymers 14:351. https://doi.org/10.3390/polym14020351
78. Liu R, Hou L, Yue G, Li H, Zhang J, Liu J, Miao B, Wang N, Bai J, Cui Z, Liu T, Zhao Y (2022) Progress of fabrication and applications of electrospun hierarchically porous nanofbers. Adv Fiber Mater 4. https://doi.org/10.1007/s42765-022-00132-z
79. Yu DG, Wang M, Ge R (2021) Strategies for sustained drug release from electrospun multi-layer nanostructures. WIREs Nanomed Nanobiotechnol 13:e1772. https://doi.org/10.1002/wnan.1772
80. Wlodarczyk J, Stojko M, Musial-Kulik M, Karpeta-Jarzabek P, Pastusiak M, Janeczek H, Dobrzynski P, Sobota M, Kasperczyk J (2022) Dual-jet electrospun PDLGA/PCU nonwovens and their mechanical and hydrolytic degradation properties. J Mech Behav Biomed 126(2):105050. https://doi.org/10.1016/j.jmbbm.2021.105050
81. Lv H, Yu DG, Wang M, Ning T (2021) Nanofabrication of Janus fibers through side-by-side electrospinning - a mini review. Mater Highlight. https://doi.org/10.2991/mathi.k.210212.001
82. Malihe G, Shahnoosh A, Amir R, Shiva R, Hajir BS (2022) Fabrication and characterization of chitosan-polycaprolactone core-shell nanofibers containing tetracycline hydrochloride. Colloid Surface A 636:128163. https://doi.org/10.1016/j.colsurfa.2021.128163
83. Abdullah MF, Andriyana A, Muhamad F, Ang BC (2021) Effect of core-to-shell flow rate ratio on morphology, crystallinity, mechanical properties and wettability of poly(lactic acid) fibers prepared via modified coaxial electrospinning. Polymer 237(12):124378. https://doi.org/10.1016/j.polymer.2021.124378

84. Kang S, Zhao K, Yu DG, Zheng X, Huang C (2022) Advances in biosensing and environmental monitoring based on electrospun nanofibers. Adv Fiber Mater 4(1). https://doi.org/10.1007/s42765-021-00129-0
85. Yang XL, Wang JW, Guo HT, Liu L, Xu WH, Duan GG (2020) Structural design toward functional materials by electrospinning: a review. e-Polymers 20(1):682–712. https://doi.org/10.1515/epoly-2020-0068
86. Kang S, Hou S, Chen X, Yu D-G, Wang L, Li X, Williams GR (2020) Energy-saving electrospinning with a concentric Teflon-core rod spinneret to create medicated nanofibers. Polymers 12(10):2421. https://doi.org/10.3390/polym12102421
87. Li Y, Wang D, Xu GC, Qiao L, Li Y, Gong HY, Shi L, Li DW, Gao M, Liu GR, Zhang JJ, Wei WH, Zhang XS, Liang X (2021) ZIF-8/PI nanofibrous membranes with high-temperature resistance for highly efficient PM0.3 air filtration and oil-water separation. Front Chem 9:810861. https://doi.org/10.3389/fchem.2021.810861
88. Na KH, Kim BS, Yoon HS, Song TH, Kim SW, Cho CH, Choi WY (2021) Fabrication and photocatalytic properties of electrospun Fe-doped TiO_2 nanofibers using polyvinyl pyrrolidone precursors. Polymers 13(16):2634. https://doi.org/10.3390/polym13162634
89. Hardt JC, Pellá MCG, Meira ACR, Rosenberger AG, Caetano J, Dragunski DC (2021) Potential wound dressings from electrospun medicated poly(butylene-adipate-co-terephthalate)/poly-(ε-caprolactone) microfibers. J Mol Liq 339(10):116694. https://doi.org/10.1016/j.molliq.2021.116694
90. Bae Y, Kim Y, Lee ES (2021) Endosomal pH-responsive Fe-based hyaluronate nanoparticles for doxorubicin delivery. Molecules 26(12):3547. https://doi.org/10.3390/molecules26123547
91. Sivan M, Madheswaran D, Valtera J, Kostakova EK, Lukas D (2021) Alternating current electrospinning: the impacts of various high-voltage signal shapes and frequencies on the spinnability and productivity of polycaprolactone nanofibers. Mater Design 213(2):110308. https://doi.org/10.1016/j.matdes.2021.110308
92. Hajjari MM, Golmakani MT, Sharif N, Niakousari M (2021) In-vitro and in-silico characterization of zein fiber incorporating cuminaldehyde. Food Bioprod Process 128(7):166–176. https://doi.org/10.1016/j.fbp.2021.05.003
93. Lee B, Song Y, Park C, Kim J, Kang J, Lee H, Yoon J, Cho S (2021) Focused patterning of electrospun nanofibers using a dielectric guide structure. Polymers 13(9):1505. https://doi.org/10.3390/polym13091505
94. Li XY, Qi WW, Zhang YX, Jiang SY, Yang B, Xiong L, Tong JC (2019) Helicid ameliorates learning and cognitive ability and activities cAMP/PKA/CREB signaling in chronic unpredictable mild stress rats. Biolog Pharm Bull 42(7):1146–1154. https://doi.org/10.1248/bpb.b19-00012
95. Tong JC, Zhou ZM, Qi WW, Jiang SY, Yang B, Zhong ZL, Jia YW, Li XY, Xiong L, Nie LW (2019) Antidepressant effect of helicid in chronic unpredictable mild stress model in rats. Int Immunopharmacol 67:13–21. https://doi.org/10.1016/j.intimp.2018.11.052
96. Mbituyimana B, Mao L, Hu S, Ullah MW, Chen K, Fu L, Zhao W, Shi Z, Yang G (2021) Bacterial cellulose/glycolic acid/glycerol composite membrane as a system to deliver glycolic acid for anti-aging treatment. J Bioresource Bioprod 6(2):129–141. https://doi.org/10.1016/j.jobab.2021.02.003
97. Joseph B, Sagarika VK, Sabu C, Kalarikkal N, Thomas S (2020) Cellulose nanocomposites: Fabrication and biomedical applications. J Bioresources Bioproducts 5(4):223–237. https://doi.org/10.1016/j.jobab.2020.10.001
98. Fatima A, Yasir S, Khan MS, Manan S, Ullah MW, Ul-Islam M (2021) Plant extract-loaded bacterial cellulose composite membrane for potential biomedical applications. J Bioresource Bioprod 6(1):26–32. https://doi.org/10.1016/j.jobab.2020.11.002